Electronic structure and thermoelectric properties of half-Heusler Zr0.5Hf0.5NiSn by first-principles calculations

ARTICLE *in* JOURNAL OF APPLIED PHYSICS · MAY 2013

Impact Factor: 2.18 · DOI: 10.1063/1.4804939

5 AUTHORS, INCLUDING:

Daifeng Zou
Hunan University of Science and Technology
7 PUBLICATIONS **48** CITATIONS

SEE PROFILE

Shang-Hang Xie
Sun Yat-Sen University
51 PUBLICATIONS **609** CITATIONS

SEE PROFILE

Yunya Liu
Xiangtan University
33 PUBLICATIONS **480** CITATIONS

SEE PROFILE

Electronic structure and thermoelectric properties of half-Heusler Zr0.5Hf0.5NiSn by first-principles calculations

D. F. Zou, S. H. Xie, Y. Y. Liu, J. G. Lin, and J. Y. Li

Citation: J. Appl. Phys. **113**, 193705 (2013); doi: 10.1063/1.4804939
View online: http://dx.doi.org/10.1063/1.4804939
View Table of Contents: http://jap.aip.org/resource/1/JAPIAU/v113/i19
Published by the American Institute of Physics.

Electronic structure and thermoelectric properties of half-Heusler $Zr_{0.5}Hf_{0.5}NiSn$ by first-principles calculations

D. F. Zou,[1] S. H. Xie,[1] Y. Y. Liu,[1,a)] J. G. Lin,[1] and J. Y. Li[2,b)]
[1]*Key Laboratory of Low Dimensional Materials and Application Technology of Ministry of Education, Faculty of Materials, Optoelectronics and Physics, Xiangtan University, Xiangtan, Hunan 411105, China*
[2]*Department of Mechanical Engineering, University of Washington, Seattle, Washington 98195-2600, USA*

(Received 22 January 2013; accepted 29 April 2013; published online 17 May 2013)

The electronic structures of $Zr_{0.5}Hf_{0.5}NiSn$ and the parent compounds ZrNiSn and HfNiSn are investigated by using first-principles calculations, and the thermoelectric properties are calculated on the base of the semi-classical Boltzmann transport theory and the empirical thermal conductivity model. The temperature dependence of thermoelectric transport properties of these three compounds is discussed and compared with experimental data, and good agreements are observed. To further optimize the thermoelectric performance of the $Zr_{0.5}Hf_{0.5}NiSn$ compound, the chemical potential dependence of electrical transport properties at three different temperatures is investigated, and the maximum power factors and corresponding optimal *p*- or *n*-type doping levels are evaluated, suggesting that the compound has better thermoelectric performance when it is *p*-type doped. © *2013 AIP Publishing LLC*. [http://dx.doi.org/10.1063/1.4804939]

I. INTRODUCTION

Thermoelectric materials have been extensively studied over the past several decades based on their ability to convert waste heat into electricity. The efficiency of a thermoelectric material at temperature T is evaluated by the dimensionless figure of merit $ZT = S^2\sigma T/\kappa$, where S is the thermopower, σ is the electrical conductivity, and κ is the thermal conductivity.[1] To obtain good thermoelectric materials, a high power factor $S^2\sigma$ and a low thermal conductivity κ must be achieved simultaneously. However, improving the thermoelectric efficiency is not easy because the different parameters entering ZT are coupled and compete with each other. As a result, one needs to search for new compounds and maximize the ZT values of them by optimizing the carrier concentration and increasing the phonon scattering.

The *M*NiSn-based (M = Ti, Zr, Hf) half-Heusler thermoelectric materials have attracted great attentions because of their large thermopower and moderate electrical conductivity.[2–13] However, one prominent problem of these compounds for thermoelectric application is their relatively high lattice thermal conductivity, which can be as high as 10 W/mK.[2–5] It was reported that substitution with isoelectronic elements in the *M*-site lattice can cause additional phonon scattering, and thus can lead to an overall reduction of the total thermal conductivity without substantial modification of electronic properties.[5–9] Among the $(M_{0.5}, M'_{0.5})NiSn$ (M, M′ = Ti, Zr, Hf) half-Heusler alloys, the highest dimensionless figure of merit ZT was achieved for the $Zr_{0.5}Hf_{0.5}NiSn$ alloy, which has the best balance between a high power factor and an effectively reduced thermal conductivity.[6] Recently, the quaternary $Zr_{0.5}Hf_{0.5}NiSn$ compound has been investigated to study the changes in the figure of merit by various substitutions.[7–11] Hohl *et al*. have reported that $\kappa = 5.4$ W/mK and $ZT = 0.5$ are achieved in Ta-doped $Zr_{0.5}Hf_{0.5}NiSn$ at 700 K.[7] It was found experimentally that Sb is an effective dopant for the Sn sites of $Zr_{0.5}Hf_{0.5}NiSn$ and can reduce the thermal conductivity to 5–6 W/mK at room temperature,[8] and the ZT value can reach 0.7 at 800 K for the spark plasma sintered $Zr_{0.5}Hf_{0.5}NiSn_{0.98}Sb_{0.02}$.[9] On the other hand, if the Ni atom is partially substituted by the Pd atom, the ZT value can be enhanced to 0.7 for the $Zr_{0.5}Hf_{0.5}Ni_{0.8}Pd_{0.2}Sn_{0.99}Sb_{0.01}$ compound.[10] Sakurada and Shutoh found that a maximum ZT of 1.5 was achieved at 700 K for Sb-doped compound $(Zr_{0.5}Hf_{0.5})_{0.5}Ti_{0.5}NiSn_{0.998}Sb_{0.002}$.[5,11] Additionally, reduced thermal conductivity and improved thermoelectric performance could be obtained in the fine-grained (Zr,Hf)NiSn based alloys[12] and single crystalline $Zr_{0.5}Hf_{0.5}NiSn$ thin film.[13]

On the theoretical side, Yang *et al*.[14] calculated the electronic transport properties of a large number of semiconducting half-Heusler compounds, including ZrNiSn and HfNiSn, using *ab initio* calculations and the Boltzmann transport equation, and estimated the optimal doping concentrations of each of the half-Heusler compounds. A theoretical survey of the thermoelectric performance of half-Heusler compounds TiNiSn and TiCoSb was carried out by Wang *et al*.[15] Chaput *et al*.[16] investigated the electronic structures of $Ti_{0.5}Hf_{0.5}NiSn$ and related half-Heusler compounds, and calculated the thermopower of these compounds with two different approximations, i.e., the constant relaxation time approximation and the constant mean free path approximation. However, the theoretical research on the thermoelectric performance of $Zr_{0.5}Hf_{0.5}NiSn$ compound is rare. In this paper, semi-classic Boltzmann transport theory is used to investigate the thermoelectric performance of the doped $Zr_{0.5}Hf_{0.5}NiSn$ which based on the electronic structures obtained from the first-principles calculations, and the results are compared with experimental data.

a)Electronic mail: yyliu@xtu.edu.cn.
b)Electronic mail: jjli@u.washington.edu.

According to the chemical potential dependence of electrical transport properties of $Zr_{0.5}Hf_{0.5}NiSn$, we estimated the optimal *p*- or *n*-type doping concentrations based on the calculated maximum power factors. Our results can offer useful guidance on how to optimize the thermoelectric properties of this compound.

II. CRYSTALLINE LATTICE AND ELECTRONIC STRUCTURE

The calculations were performed using the projector augment wave methods as implemented in the Vienna *ab initio* Simulation Package (VASP).[17–19] The exchange-correlation energy was in the form of Perdew–Burke–Ernzerhof with generalized gradient approximations (GGA).[20] The energy convergence criterion was chosen to be 10^{-6} eV and the cut-off energy of the plane-wave was set to 400 eV. It has been reported that there is only a small effect on the band structure of ZrNiSn if spin-orbit interaction is included,[21] e.g., minor splitting of the degenerate bands and a small reduction of the band gap with no change in the shape of the band structure of the lowest conduction band or highest valence band, and it is found that the effect of spin-orbit interaction on the transport properties of half-Heusler compounds is negligible.[22] Therefore, the spin-orbit coupling effect is neglected for simplicity in this paper.

The half-Heusler *M*NiSn (M = Zr, Hf) compounds are some of the better known compounds in the cubic MgAgAs-type structure with the space group $F\bar{4}3m$. Each of the compounds can be represented as four interpenetrating face-centered cubic (FCC) sublattices: The crystallographic 4*c* site (1/4, 1/4, 1/4) is occupied by Zr/Hf, while the 4*a* site (0, 0, 0) and 4*d* site (3/4, 3/4, 3/4) are occupied by Ni and Sn, respectively. The conventional cell of the typical ZrNiSn is shown in Fig. 1(a). To simulate the $Zr_{0.5}Hf_{0.5}NiSn$ compound, two of the four Zr atoms in ZrNiSn unit cell are substituted by Hf atoms. The primitive cell of $Zr_{0.5}Hf_{0.5}NiSn$ contains six atoms and has a tetragonal structure with space group $P\bar{4}m2$, as shown in Fig. 1(b). The ground state lattice constant was calculated with relaxation of both atomic positions and lattice parameters. The optimized lattice constants of $Zr_{0.5}Hf_{0.5}NiSn$, along with ZrNiSn and HfNiSn, are listed in Table I together with those experimental data.[23] The calculated values for ZrNiSn and HfNiSn shown in Table I overestimate the lattice constants within 1% compared with

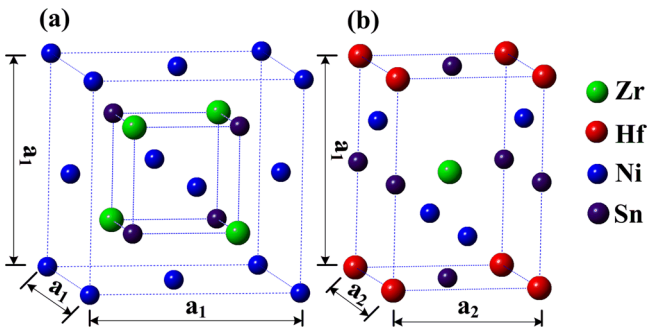

FIG. 1. (a) The conventional cell of ZrNiSn and (b) the primitive cell of $Zr_{0.5}Hf_{0.5}NiSn$.

TABLE I. Lattice constants and band gaps of ZrNiSn, HfNiSn, and $Zr_{0.5}Hf_{0.5}NiSn$.

	a_1^{Cal} (Å)	a_1^{Exp} (Å)	Gap^{Cal} (eV)	Gap^{Exp} (eV)
ZrNiSn	6.162	6.110[a]	0.52	0.18[b]
HfNiSn	6.120	6.066[a]	0.36	0.22[b]
$Zr_{0.5}Hf_{0.5}NiSn$	6.140	…	0.43	0.24[c]

[a]Reference 23.
[b]Reference 26.
[c]Reference 27.

experimental reported[23] 6.110 and 6.066 Å due to the fact that GGA often overestimates lattice constants of solids.[24] The lattice constant of ZrNiSn or HfNiSn is equivalent to the *c* axis (a_1) of the tetragonal cell for $Zr_{0.5}Hf_{0.5}NiSn$. At equilibrium state the calculated lattice constant a_1 of $Zr_{0.5}Hf_{0.5}NiSn$ is 6.140 Å, and the value falls in between those for ZrNiSn and HfNiSn. We conclude that the calculated lattice constant of $Zr_{0.5}Hf_{0.5}NiSn$ obeys Vegard's law[25] based on a continuous change of lattice constant though the substitution of Zr by Hf, as shown in Table I.

The calculated electronic band structures of ZrNiSn, HfNiSn, and $Zr_{0.5}Hf_{0.5}NiSn$ are shown in Fig. 2. It can be seen that the $Zr_{0.5}Hf_{0.5}NiSn$ has a direct gap at the Γ point from Fig. 2(c), while the two parent compounds, ZrNiSn and HfNiSn, have indirect gaps between the Γ point and the X point as shown in Figs. 2(a) and 2(b). This is believed to be caused by the folding of bands when going from face-centered cubic to simple tetragonal cell, since the ΓX vector of the face-centered cubic belongs to the reciprocal lattice of the simple tetragonal cell at the Brillouin-zone.[16] The calculated energy band gaps are 0.525 eV for ZrNiSn and 0.365 eV for HfNiSn. These values are in good agreement with those theoretical calculations reported previously.[14] The experimental measured energy gaps are 0.18 eV and 0.22 eV for ZrNiSn and HfNiSn, respectively.[26] The band gap of $Zr_{0.5}Hf_{0.5}NiSn$ is found to be 0.43 eV, which is much larger than the experimental value 0.24 eV.[27] It is well known that GGA often underestimates the band gaps of semiconductors.[28] In this work, the calculated band gaps are larger than those measured values, and such behavior can be explained from the fact that the band gaps will shrink due to structural imperfections,[29,30] such as antisite defects, which are the inherent features of half-Heusler compounds,[31] while in our calculations the band gaps were estimated only for perfect single crystals. It was reported that the shape of the band structure is correct and the problem of band gap can be amended by a rigid shift of the conduction band.[32] In Secs. III–V, we correct this problem by a shift of the conductional band to the experiment values in order to obtain more realistic thermoelectric properties.

III. THERMOPOWER AND ELECTRICAL CONDUCTIVITY

The thermopower *S* and electronic conductivity σ were obtained by using the semi-classical Boltzmann theory in conjunction with rigid band and constant relaxation time

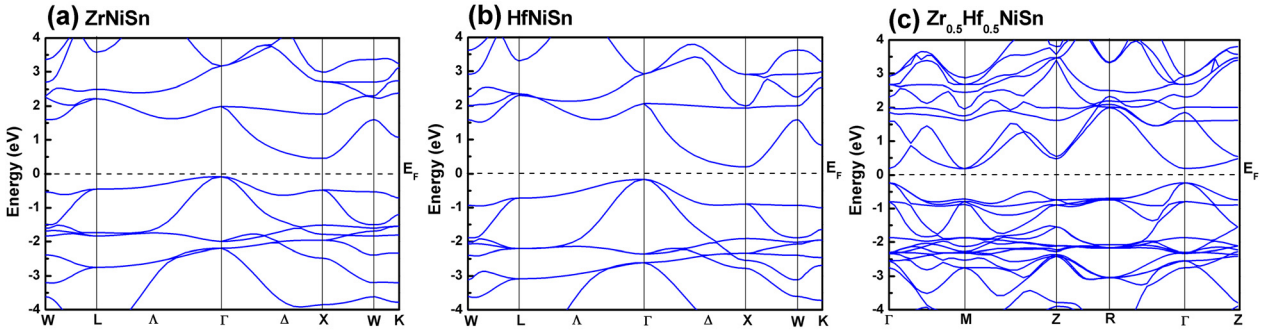

FIG. 2. The band structures for (a) ZrNiSn, (b) HfNiSn, and (c) $Zr_{0.5}Hf_{0.5}NiSn$. The Fermi level is set to be zero.

approximations.[33] All the calculations of transport properties were implemented in the BoltzTraP package,[33] and the necessary crystal structures and eigen-energies for BoltzTraP calculation were obtained from VASP results. In order to get reasonable transport properties, we calculated the eigen-energies using a $31 \times 31 \times 22$ $\boldsymbol{k}$-point sampling for $Zr_{0.5}Hf_{0.5}NiSn$ and $31 \times 31 \times 31$ $\boldsymbol{k}$-point grid for ZrNiSn and HfNiSn which were generated by the Monkhorst-Pack scheme.

In order to compare the thermoelectric properties of $Zr_{0.5}Hf_{0.5}NiSn$ and the parent compounds ZrNiSn and HfNiSn, the thermopower S and electrical conductivity σ of ZrNiSn, HfNiSn and $Zr_{0.5}Hf_{0.5}NiSn$ as a function of temperature are shown in Figs. 3(a) and 3(b). Here, we only calculate transport coefficients for the 1% n-type doping of ZrNiSn and $Zr_{0.5}Hf_{0.5}NiSn$ and 2% n doping of HfNiSn since these doping concentrations have been studied experimentally. In order to fit the experimental thermopower, we assume that the carrier concentration of 1% n-type doped ZrNiSn and $Zr_{0.5}Hf_{0.5}NiSn$ is $2.0 \times 10^{20}\,cm^{-3}$ and $3.0 \times 10^{20}\,cm^{-3}$, which are slightly higher than the theoretical carrier concentrations (1% doped ZrNiSn: $1.70 \times 10^{20}\,cm^{-3}$; 1% doped $Zr_{0.5}Hf_{0.5}NiSn$: $1.72 \times 10^{20}\,cm^{-3}$). The carrier concentration of HfNiSn is adopted to experimental measured $7.23 \times 10^{20}\,cm^{-3}$ which comes from Ref. 9. The computed thermopower of ZrNiSn, HfNiSn and $Zr_{0.5}Hf_{0.5}NiSn$ agrees well with those observed in experiments,[5,9,10] as shown in Fig. 3(a). Within the framework of the Boltzmann transport equation in constant relaxation time (τ) approximation, the electrical conductivity (σ) is expressed in the form of the ratio σ/τ. To calculate the electrical conductivity σ values of the three doped compounds, we must determine the relaxation time τ. Here, we adopt the strategy previously used by Ong *et al.* for calculating the thermoelectric properties of ZnO.[34] We assume that the relaxation time τ is direction independent, and treat relaxation time as a constant at a certain specific temperature and carrier concentration. The reported experimental conductivity for 1% Sb-doped $Zr_{0.5}Hf_{0.5}NiSn_{0.99}Sb_{0.01}$ is 0.855 mΩ cm at 730 K,[5] which combined with the calculated σ/τ yields $\tau = 1.21 \times 10^{-13}$ s for this sample. Inserting these values into the standard electron-phonon dependence on T and n for τ, namely, $\tau = CT^{-1}n^{-1/3}$, we can determine that the constant $Cn^{-1/3}$ amounts to 8.87×10^{-12} s K. Then, we can calculate electrical conductivity σ as $\sigma/\tau \times (8.87 \times 10^{-12}\ T^{-1})$ with τ in s and T in K. According to the same strategy, the relaxation time τ of 1% doped ZrNiSn and 2% doped HfNiSn is 6.09×10^{-13} s and 5.16×10^{-13} s, respectively. The calculated electrical conductivity of ZrNiSn, HfNiSn and $Zr_{0.5}Hf_{0.5}NiSn$ is shown in Fig. 3(b). The results follow the trend that the electrical conductivity decreases with increasing temperature and it exhibits metal-like behavior.

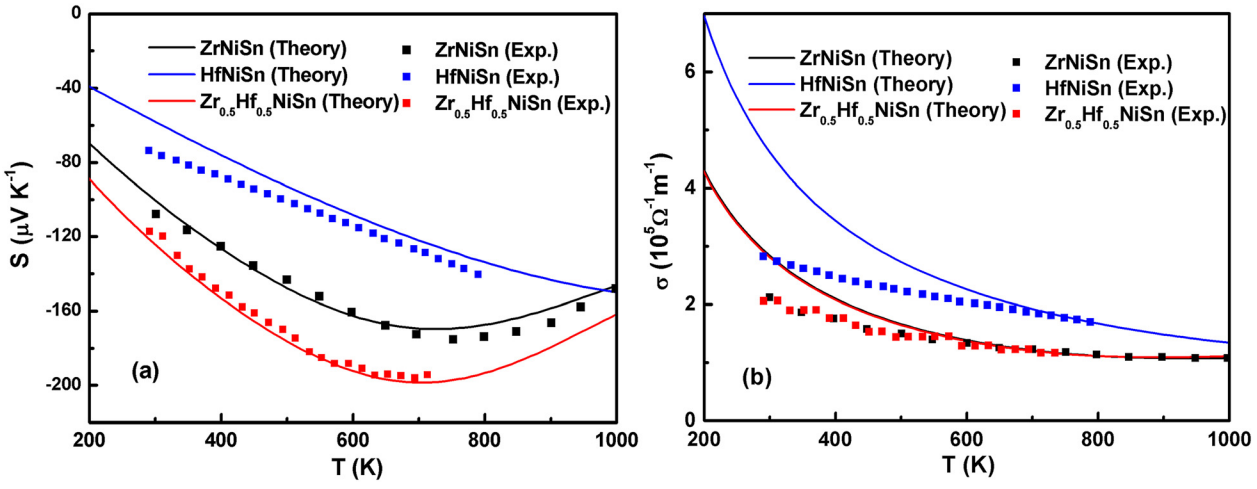

FIG. 3. Calculated (a) thermopower S and (b) electrical conductivity σ for doped ZrNiSn, HfNiSn, and $Zr_{0.5}Hf_{0.5}NiSn$ compounds as a function of temperature. The corresponding experimental results[5,9,10] are displayed together for comparison.

Agreement with experiment is good at high-temperature regime, while the electrical conductivity of the three compounds deviates from experimental observations in the low-temperature regime. This is not surprising since the electrical conductivity is computed under the constant relaxation time approximation. From Fig. 3(b), it can be seen that 1% doped ZrNiSn and $Zr_{0.5}Hf_{0.5}NiSn$ possess the comparable values of electrical conductivity, and it is because substitution with isoelectronic elements in the *M*-site of $Zr_{0.5}Hf_{0.5}NiSn$ can only cause mass disorder while does not substantially modify the electronic properties.

IV. THERMAL CONDUCTIVITY AND *ZT*

In order to evaluate the figure of merit *ZT*, one should obtain the total thermal conductivity κ which can be separated into the lattice thermal conductivity (κ_l), electronic thermal conductivity (κ_e), and bipolar thermal conductivity (κ_b) contributions.[35] The lattice thermal conductivity κ_l of half-Heusler from first principle was investigated by Shiomi *et al.*[36] They confirmed that κ_l obey Umklapp phonon scattering $1/T$ behavior between 100 K and 1000 K. The electronic part of the thermal conductivity is given by Wiedemann-Tranz law, $\kappa_e = L\sigma T$, where L is the calculated carrier-concentration-dependent Lorenz number, σ is the electrical conductivity and T is the absolute temperature. The bipolar thermal conductivity can be expressed as $\kappa_b = T\sum\sigma_i\sigma_j(S_i - S_j)^2/2$, where T is the temperature, σ is the electrical conductivity, and S is the thermopower.[35] A very good description of the experimental data can be obtained using the functional form $\kappa = A/T + BT + C$ for the total thermal conductivity. The first term A/T indicates the contribution of the lattice thermal conductivity, with $A = 3204$ W/m, 967 W/m and 720 W/m for ZrNiSn, HfNiSn and $Zr_{0.5}Hf_{0.5}NiSn$, respectively. The second term BT stands for the contributions of electronic and bipolar thermal conductivity, and the fitted B values are 0.0048 W/mK^2, 0.0010 W/mK^2 and 0.0012 W/mK^2 for ZrNiSn, HfNiSn and $Zr_{0.5}Hf_{0.5}NiSn$, respectively. The C is only a fitted constant. The values of B are much less than that of A, and it is reasonable that the sum of the electronic and bipolar thermal conductivity contributes less to the total thermal conductivity compared to lattice thermal conductivity. The fitted thermal conductivity κ values are plotted in Fig. 4(a). The fitted results of the thermal conductivity for the three compounds show good match with the experimental data.[5,9,10] As we can see from Fig. 4(a), the substitution with isoelectronic elements in the *M*-site effectively decreases the total thermal conductivity, and it attributes to mass fluctuation scattering as the prominent scattering mechanism of $Zr_{0.5}Hf_{0.5}NiSn$, which is caused by a large difference in atomic masses of Zr (91 g/mol) and Hf (178 g/mol).[3] The calculated *ZT* values along with the experimental data are shown in Fig. 4(b); the calculations confirm the experimental observations that the *ZT* value is greatly enhanced due to the reduced the lattice thermal conductivity by the substitution of isoelectronic elements in the *M*-site.

V. TRANSPORT PROPERTIES OF $Zr_{0.5}Hf_{0.5}NiSn$

In order to further improve the thermoelectric performance of $Zr_{0.5}Hf_{0.5}NiSn$ compound, one needs to maximize the power factor. The chemical potential dependence of the electrical transport properties of $Zr_{0.5}Hf_{0.5}NiSn$ was calculated at three different temperatures: 300, 500, and 700 K, as shown in Fig. 5. Within the rigid-band shift model, the chemical potential μ determines the carrier concentration of the compound. In the case of *n*-type doping, the Fermi level gets up-shifted, which corresponds to positive chemical potential. For *p*-type doping, the Fermi level shifts down and the corresponding chemical potential is negative. As seen in Figs. 5(a) and 5(b), the thermopower S value is large around the low chemical potential μ, while the power factor $S^2\sigma/\tau$ is small due to low carrier concentration. As can be seen from Fig. 5(b), there are several peaks within the considered chemical potential range for three different temperatures, which suggests that the thermoelectric performance of the $Zr_{0.5}Hf_{0.5}NiSn$ compound can be optimized by appropriate doping concentration. At 700 K, there are two peaks in the vicinity of the Fermi level which are located at $\mu = -0.22$ eV

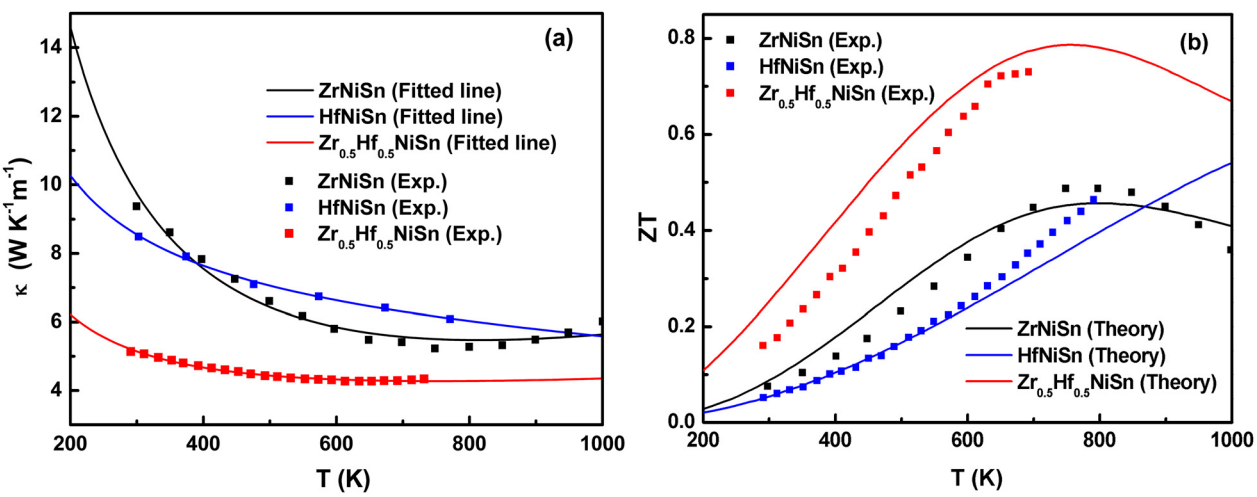

FIG. 4. (a) Temperature dependence of thermal conductivity κ of doped ZrNiSn, HfNiSn and $Zr_{0.5}Hf_{0.5}NiSn$ compounds fitted by $\kappa = A/T + BT + C$, where A, B and C are fitted values and T is the absolute temperature. The solid squares are the experimental data.[5,9,10] (b) The corresponding calculated figure of merit *ZT*.

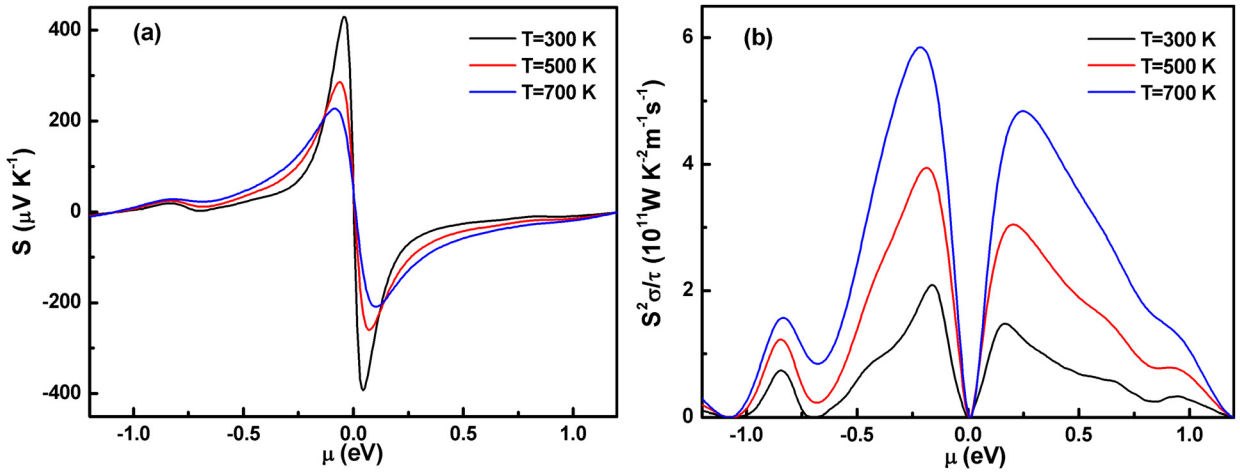

FIG. 5. Chemical potential dependence of (a) thermopower S and (b) power factor over relaxation time $S^2\sigma/\tau$ of $Zr_{0.5}Hf_{0.5}NiSn$ at 300 K, 500 K, and 700 K.

and $\mu = 0.25$ eV. The corresponding thermoelectric power factors are 5.85×10^{11} W K^{-2} m^{-1} s^{-1} at -0.22 eV, and 4.85×10^{11} W K^{-2} m^{-1} s^{-1} at 0.25 eV. Besides the electrical transport parameters, we have also calculated the optimal carrier concentration in terms of chemical potential for each temperature T by using[37]

$$n = \int D(\varepsilon) \frac{1}{e^{(\mu-\varepsilon)/k_B T} + 1} d\varepsilon, \quad (1)$$

where n, ε, and D are the carrier concentration, energy, and density of states, respectively. The calculated carrier concentrations are 1.11×10^{21} cm^{-3} and 6.47×10^{20} cm^{-3} at 700 K for p- and n-type doping of $Zr_{0.5}Hf_{0.5}NiSn$, respectively. The two peaks around the Fermi level move to a slightly larger number of chemical potential with temperature decreased from 700 K to 300 K, and there are significant decreases in the power factors. The results are summarized in Table II, which gives the optimal carrier concentrations and the corresponding chemical potential of $Zr_{0.5}Hf_{0.5}NiSn$ at three different temperatures in Fig. 5(b). Combining the optimum doping concentrations shown in Table II, it is possible to further improve the thermoelectric performance of $Zr_{0.5}Hf_{0.5}NiSn$ using many other possible atoms doping at the Zr/Hf, Ni, and Sn sites.

To further assess the thermoelectric performance of $Zr_{0.5}Hf_{0.5}NiSn$ at the optimum doping concentrations, the thermopower S and power factor over relaxation time $S^2\sigma/\tau$ of $Zr_{0.5}Hf_{0.5}NiSn$ as a function of temperature are shown in Figs. 6(a)–6(d). These concentrations can be easily achieved experimentally by substituting within 6.5% of a dopant, assuming that each dopant donates one hole or electron and all the doped holes appear as charge carriers.[22] As can be seen in Figs. 6(a) and 6(b), the thermopower S of $Zr_{0.5}Hf_{0.5}NiSn$ compound decreases with increase in carrier concentration. As for the low carrier concentration (2.57×10^{20} cm^{-3} for p-type and 1.62×10^{20} cm^{-3} for n-type), the magnitude of thermopower S first increases with increasing temperature until reaching a maximum, and then decreases due to the bipolar effect. This tendency of n-type doping is consistent with experimental phenomena.[5,10] However, the analysis of p-type is difficult because there are no experimental data available. As shown in Figs. 6(c) and 6(d), the p-type $Zr_{0.5}Hf_{0.5}NiSn$ exhibits a higher value of power factor over relaxation time $S^2\sigma/\tau$ at the optimal carrier concentrations compared with the corresponding n-type. The $Zr_{0.5}Hf_{0.5}NiSn$ compound has been found to exhibit inherent n-type semiconducting behavior at room temperature. Recently, some p-type half-Heusler compounds are reported by introducing acceptor dopants which can change the major carriers from electrons to holes.[38–41] It is significant to explore the p-type doping of $Zr_{0.5}Hf_{0.5}NiSn$ in experiment which can be produced by introducing holes into the system at the Zr/Hf, Ni, and/or Sn sites. As for the n-type $Zr_{0.5}Hf_{0.5}NiSn$, the optimal doping level at the considered temperatures is in the range from 1.62×10^{20} cm^{-3} to 6.47×10^{20} cm^{-3}, and it can be seen from Fig. 6(d) that the power factor over relaxation time $S^2\sigma/\tau$ increases with increased carrier concentration at medium-high temperature. Because the experimental data of thermal conductivity are not available, we cannot determine the ZT value of these doping levels for $Zr_{0.5}Hf_{0.5}NiSn$ compound. According to the range of optimal doping concentration, the highest ZT values of $Zr_{0.5}Hf_{0.5}NiSn$ can be achieved experimentally by finding out the best balance between power factor and thermal conductivity. So, there is still much room in experiment for further improving the thermoelectric properties of $Zr_{0.5}Hf_{0.5}NiSn$ compound.

TABLE II. Peak values of power factors with respect to relaxation time $S^2\sigma/\tau$ and their corresponding thermopower S at 300 K, 500 K, and 700 K as a function of chemical potential μ around the Fermi level. The optimal doping carrier concentrations n corresponding to chemical potential μ are also listed.

	300 K		500 K		700 K	
	p-type	n-type	p-type	n-type	p-type	n-type
S (μV K^{-1})	165	−145	155	−137	141	−130
$S^2\sigma/\tau$ (10^{11} W K^{-2} m^{-1} s^{-1})	2.07	1.47	3.93	3.04	5.84	4.84
μ (eV)	−0.15	0.16	−0.18	0.20	−0.22	0.25
n (10^{20} cm^{-3})	2.57	−1.62	6.20	−3.45	11.10	−6.47

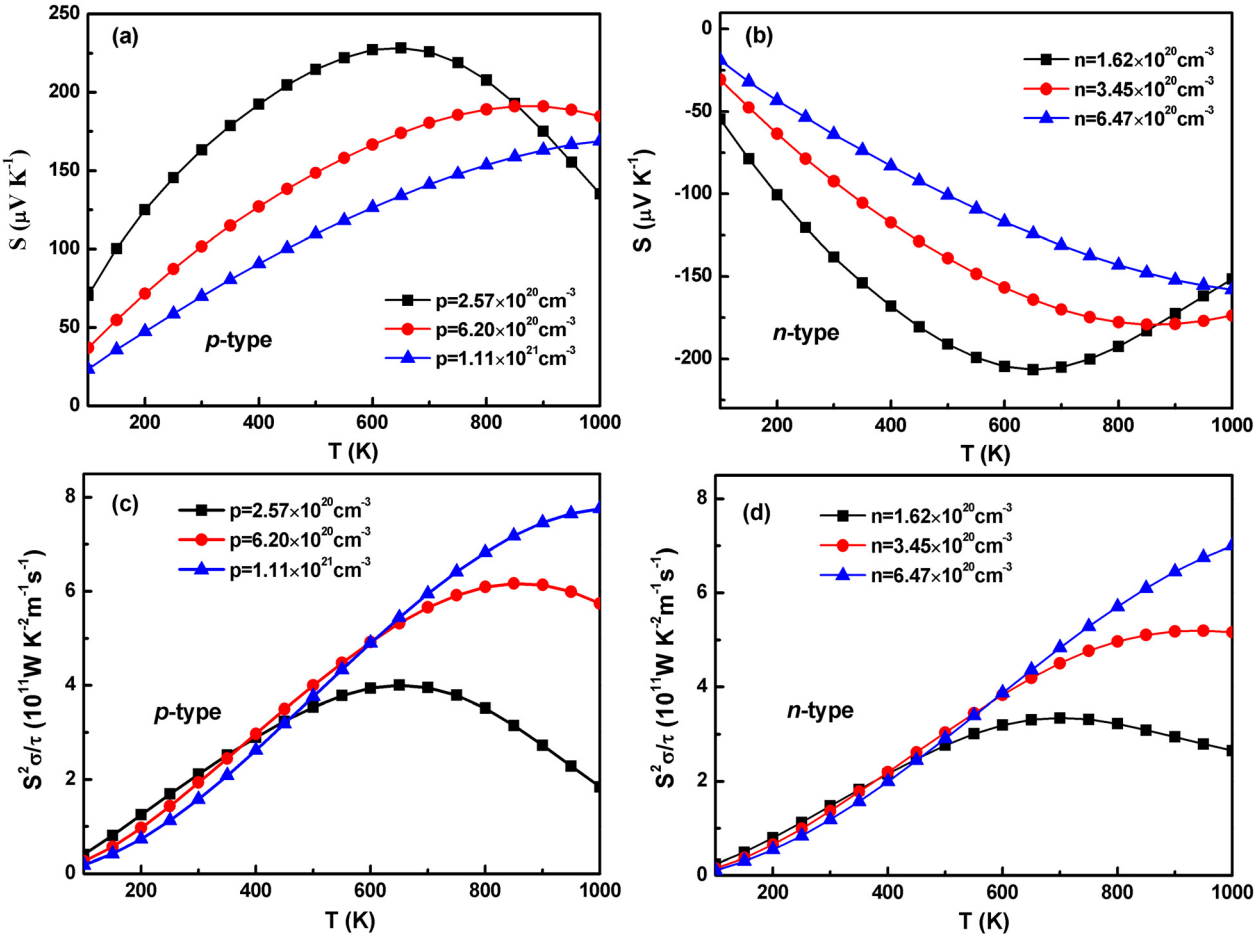

FIG. 6. Temperature dependence of transport properties of $Zr_{0.5}Hf_{0.5}NiSn$ at the optimal doping carrier concentrations. (a) *p*-type thermopower *S*. (b) *n*-type thermopower *S*. (c) *p*-type power factors with respect to relaxation time $S^2\sigma/\tau$. (d) *n*-type power factors with respect to relaxation time $S^2\sigma/\tau$.

VI. CONCLUSIONS

In summary, we have presented the electronic and transport properties of $Zr_{0.5}Hf_{0.5}NiSn$ and the parent compounds ZrNiSn and HfNiSn by first-principles electronic structure calculations in conjunction with the semi-classical Boltzmann theory, and the results are discussed and compared with experimental data with good agreement. Based on the calculated thermopower and power factor of $Zr_{0.5}Hf_{0.5}NiSn$ as a function of chemical potential, the maximum power factors and the corresponding optimal doping concentrations are estimated, and it can offer useful guidelines for tuning the doping levels and composition to improve the thermoelectric performance of this compound.

ACKNOWLEDGMENTS

This work was supported by Natural Science Foundation of China (Approval Nos. 11172255 and 51172189) and US National Science Foundation (CMMI-1235535).

[1]G. J. Snyder and E. S. Toberer, Nature Mater. **7**, 105 (2008).
[2]S. R. Culp, S. J. Poon, N. Hickman, T. M. Tritt, and J. Blumm, Appl. Phys. Lett. **88**, 042106 (2006).
[3]S. Bhattacharya, M. Skove, M. Russell, T. Tritt, Y. Xia, V. Ponnambalam, S. Poon, and N. Thadhani, Phys. Rev. B **77**, 184203 (2008).
[4]S. Ouardi, G. H. Fecher, C. Felser, C. G. F. Blum, D. Bombor, C. Hess, S. Wurmehl, B. Büchner, and E. Ikenaga, Appl. Phys. Lett. **99**, 152112 (2011).
[5]S. Sakurada and N. Shutoh, Appl. Phys. Lett. **86**, 082105 (2005).
[6]Y. Kimura, H. Ueno, and Y. Mishima, J. Electron. Mater. **38**, 934 (2009).
[7]H. Hohl, A. P. Ramirez, C. Goldmann, G. Ernst, B. Wölfing, and E. Bucher, J. Phys.: Condens. Matter **11**, 1697 (1999).
[8]C. Uher, J. Yang, S. Hu, D. T. Morelli, and G. P. Meisner, Phys. Rev. B **59**, 8615 (1999).
[9]C. Yu, T. J. Zhu, R. Z. Shi, Y. Zhang, X. B. Zhao, and J. He, Acta Mater. **57**, 2757 (2009).
[10]Q. Shen, L. Chen, T. Goto, T. Hirai, J. Yang, G. P. Meisner, and C. Uher, Appl. Phys. Lett. **79**, 4165 (2001).
[11]N. Shutoh and S. Sakurada, J. Alloys Compd. **389**, 204 (2005).
[12]H. H. Xie, C. Yu, T. J. Zhu, C. G. Fu, G. J. Snyder, and X. B. Zhao, Appl. Phys. Lett. **100**, 254104 (2012).
[13]T. Jaeger, C. Mix, M. Schwall, X. Kozina, J. Barth, B. Balke, M. Finsterbusch, Y. U. Idzerda, C. Felser, and G. Jakob, Thin Solid Films **520**, 1010 (2011).
[14]J. Yang, H. Li, T. Wu, W. Zhang, L. Chen, and J. Yang, Adv. Funct. Mater. **18**, 2880 (2008).
[15]L. L. Wang, L. Miao, Z. Y. Wang, W. Wei, R. Xiong, H. J. Liu, J. Shi, and X. F. Tang, J. Appl. Phys. **105**, 013709 (2009).
[16]L. Chaput, J. Tobola, P. Pécheur, and H. Scherrer, Phys. Rev. B **73**, 045121 (2006).
[17]G. Kresse and J. Furthmüller, Comput. Mater. Sci. **6**, 15 (1996).
[18]G. Kresse and J. Furthmüller, Phys. Rev. B **54**, 011169 (1996).
[19]G. Kresse and J. Hafner, Phys. Rev. B **47**, 558 (1993).
[20]J. P. Perdew, K. Burke, and M. Ernzerhof, Phys. Rev. Lett. **77**, 3865 (1996).
[21]P. Larson, S. Mahanti, J. Salvador, and M. Kanatzidis, Phys. Rev. B **74**, 035111 (2006).

[22]M. S. Lee, F. P. Poudeu, and S. D. Mahanti, Phys. Rev. B **83**, 085204 (2011).
[23]S. Öğüt and K. M. Rabe, Phys. Rev. B **51**, 10443 (1995).
[24]A. Khein, D. J. Singh, and C. J. Umrigar, Phys. Rev. B **51**, 4105 (1995).
[25]A. R. Denton and N. W. Ashcroft, Phys. Rev. A **43**, 3161 (1991).
[26]F. G. Aliev, N. B. Brandt, V. V. Moshchalkov, V. V. Kozyrkov, R. V. Skolozdra, and A. I. Belogorokhov, Z. Phys. B **75**, 167 (1989).
[27]B. A. Cook, G. P. Meisner, J. Yang, and C. Uher, in *Proceedings of the 18th International Conference on Thermoelectrics, IEEE Catalog No. 99TH8407* (IEEE, Piscataway, NJ, 1999), p. 64.
[28]W. G. Aulbur, L. Jönsson, and J. W. Wilkins, Solid State Phys. **54**, 1 (1999).
[29]L. F. Mattheiss, Phys. Rev. B **43**, 1863 (1991).
[30]J. W. Simonson and S. J. Poon, J. Phys.: Condens. Matter **20**, 255220 (2008).
[31]P. Qiu, J. Yang, X. Huang, X. Chen, and L. Chen, Appl. Phys. Lett. **96**, 152105 (2010).
[32]L. Xi, Y. Zhang, X. Shi, J. Yang, L. Chen, W. Zhang, J. Yang, and D. Singh, Phys. Rev. B **86**, 155201 (2012).
[33]G. K. H. Madsen and D. J. Singh, Comput. Phys. Commun. **175**, 67 (2006).
[34]K. Ong, D. Singh, and P. Wu, Phys. Rev. B **83**, 115110 (2011).
[35]N. Satyala and D. Vashaee, J. Electron. Mater. **41**, 1785 (2012).
[36]J. Shiomi, K. Esfarjani, and G. Chen, Phys. Rev. B **84**, 104302 (2011).
[37]C. Sevik and T. Cagin, Appl. Phys. Lett. **95**, 112105 (2009).
[38]H. H. Xie, C. Yu, B. He, T. J. Zhu, and X. B. Zhao, J. Electron. Mater. **41**, 1826 (2012).
[39]N. J. Takas, P. Sahoo, D. Misra, H. Zhao, N. L. Henderson, K. Stokes, and P. F. P. Poudeu, J. Electron. Mater. **40**, 662 (2011).
[40]X. Yan, G. Joshi, W. Liu, Y. Lan, H. Wang, S. Lee, J. W. Simonson, S. J. Poon, T. M. Tritt, G. Chen, and Z. F. Ren, Nano Lett. **11**, 556 (2011).
[41]P. Maji, N. J. Takas, D. K. Misra, H. Gabrisch, K. Stokes, and P. F. P. Poudeu, J. Solid State Chem. **183**, 1120 (2010).